

# Learning Efficient Tensor Representations with Ring Structure Networks

Qibin Zhao<sup>1</sup>, Masashi Sugiyama<sup>1</sup>, and Andrzej Cichocki<sup>2</sup>

<sup>1</sup>RIKEN AIP, Tokyo, Japan

<sup>2</sup>RIKEN BSI, Saitama, Japan

## Abstract

*Tensor train (TT) decomposition* is a powerful representation for high-order tensors, which has been successfully applied to various machine learning tasks in recent years. However, since the tensor product is not commutative, permutation of data dimensions makes solutions and TT-ranks of TT decomposition inconsistent. To alleviate this problem, we propose a permutation symmetric network structure by employing circular multilinear products over a sequence of low-order core tensors. This network structure can be graphically interpreted as a cyclic interconnection of tensors, and thus we call it *tensor ring (TR) representation*. We develop several efficient algorithms to learn TR representation with adaptive TR-ranks by employing low-rank approximations. Furthermore, mathematical properties are investigated, which enables us to perform basic operations in a computationally efficient way by using TR representations. Experimental results on synthetic signals and real-world datasets demonstrate that the proposed TR network is more expressive and consistently informative than existing TT networks.

## 1 Introduction

*Tensor decompositions* aim to represent a higher-order (or multi-dimensional) data as a multilinear product of several latent factors, which attracted considerable attentions in machine learning [1, 2, 3] and signal processing [4, 5] in recent years. For a  $d$ th-order “square” tensor of size  $n$  with “square” core tensor of size  $r$ , standard tensor decompositions are the *canonical polyadic (CP) decomposition* [6, 7, 8] which represents data as a sum of rank-one tensors by  $\mathcal{O}(dnr)$  parameters and *Tucker decomposition* [9, 10, 11, 12] which represents data as a core tensor and several factor matrices by  $\mathcal{O}(dnr + r^d)$  parameters. In general, CP decomposition provides a compact representation but with difficulties in finding the optimal solution, while Tucker decomposition is stable and flexible but its number of parameters scales exponentially to the tensor order.

Recently, *tensor networks* have emerged as a powerful tool for analyzing very high-order tensors [13]. A powerful tensor network is *tensor train / matrix product states (TT/MPS)* representation [14], which requires  $\mathcal{O}(dnr^2)$  parameters and avoid the curse of dimensionality through a particular geometry of low-order contracted tensors. TT representation has been applied to model weight parameters in deep neural network and nonlinear kernel learning [15, 16], achieving a significant compression factor and scalability. It also has been successfully used for feature learning and classification [17]. It was shown in [18] that TT decomposition with minimal possible compression ranks always exists and can be computed by a sequence of singular value decompositions (SVDs), or by the cross approximation algorithm.

Although TT decomposition has gained a success in tackling various machine learning tasks, there are some major limitations including that i) the constraint on TT-ranks, i.e.,  $r_1 = r_{d+1} = 1$ , leads to the limited representation ability and flexibility; ii) TT-ranks are small in the border cores and large in the middle cores, which might not be optimal for a given data tensor; iii) the permutation of data tensor will yield an inconsistent solution, i.e., TT representations and TT-ranks are sensitive to the order of tensor dimensions. Hence, finding the optimal permutation remains a challenging problem.

By taking into account these limitations of TT decomposition, we introduce a new structure of tensor networks, which can be considered as a generalization of TT representations. First of all, we relax the

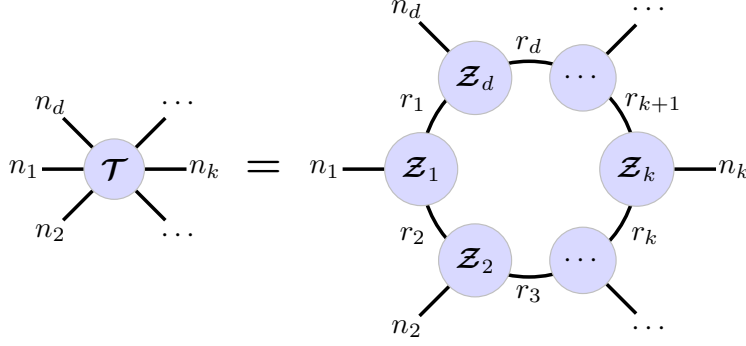


Figure 1: A graphical representation of tensor ring decomposition.

condition over TT-ranks, i.e.,  $r_1 = r_{d+1} = 1$ , leading to an enhanced representation ability. Secondly, the strict ordering of multilinear products between cores should be alleviated. Third, the cores should be treated equivalently by making the model symmetric. To this end, we add a new connection between the first and the last core tensors, yielding a circular tensor products of a set of cores. More specifically, we consider that each tensor element is approximated by performing a trace operation over the sequential multilinear products of cores. Since the trace operation ensures a scalar output,  $r_1 = r_{d+1} = 1$  is not necessary. In addition, the cores can be circularly shifted and treated equivalently due to the properties of the trace operation. By using the graphical illustration (see Fig. 1), this concept implies that the cores are interconnected circularly, which looks like a ring structure. Hence, we call this model *tensor ring (TR) decomposition* and its cores *tensor ring (TR) representations*.

To learn TR representations, we firstly develop a non-iterative TR-SVD algorithm that is computationally efficient and scalable. To obtain a low-rank TT representation, we also develop a block-wise alternating least-squares (ALS) algorithm, which updates the tensor products of two adjacent cores first; then a low-rank approximation is employed to separate this term into two cores with the lowest rank. We experimentally demonstrate the usefulness of the proposed approach on both synthetic and real-world datasets.

## 2 Tensor Ring Decomposition

The TR decomposition aims to represent a high-order (or multi-dimensional) tensor by a sequence of 3rd-order tensors that are multiplied circularly. Specifically, let  $\mathcal{T}$  be a  $d$ th-order tensor of size  $n_1 \times n_2 \times \dots \times n_d$ , denoted by  $\mathcal{T} \in \mathbb{R}^{n_1 \times \dots \times n_d}$ , TR representation is to decompose it into a sequence of latent tensors  $\mathbf{Z}_k \in \mathbb{R}^{r_k \times n_k \times r_{k+1}}$ ,  $k = 1, 2, \dots, d$ , which can be expressed in an element-wise form given by

$$T(i_1, i_2, \dots, i_d) = \text{Tr} \{ \mathbf{Z}_1(i_1) \mathbf{Z}_2(i_2) \cdots \mathbf{Z}_d(i_d) \} = \text{Tr} \left\{ \prod_{k=1}^d \mathbf{z}_k(i_k) \right\}. \quad (1)$$

$T(i_1, i_2, \dots, i_d)$  denotes the  $(i_1, i_2, \dots, i_d)$ th element of the tensor.  $\mathbf{Z}_k(i_k)$  denotes the  $i_k$ th lateral slice matrix of the latent tensor  $\mathbf{Z}_k$ , which is of size  $r_k \times r_{k+1}$ . Note that any two adjacent latent tensors,  $\mathbf{Z}_k$  and  $\mathbf{Z}_{k+1}$ , have a common dimension  $r_{k+1}$  on their corresponding modes. The last latent tensor  $\mathbf{Z}_d$  is of size  $r_d \times n_d \times r_1$ , i.e.,  $r_{d+1} = r_1$ , which ensures the product of these matrices is a square matrix. These prerequisites play key roles in TR decomposition, resulting in some important numerical properties. For simplicity, the latent tensor  $\mathbf{Z}_k$  can also be called the  $k$ th-core (or *node*). The size of cores,  $r_k, k = 1, 2, \dots, d$ , collected and denoted by a vector  $\mathbf{r} = [r_1, r_2, \dots, r_d]^T$ , are called *TR-ranks*. From (1), we can observe that  $T(i_1, i_2, \dots, i_d)$  is equivalent to the trace of a sequential product of matrices  $\{\mathbf{z}_k(i_k)\}$ . Based on (1), we can also express TR decomposition in the tensor form, given by

$$\mathcal{T} = \sum_{\alpha_1, \dots, \alpha_d=1}^{r_1, \dots, r_d} \mathbf{z}_1(\alpha_1, \alpha_2) \circ \mathbf{z}_2(\alpha_2, \alpha_3) \circ \dots \circ \mathbf{z}_d(\alpha_d, \alpha_1),$$

where the symbol ‘ $\circ$ ’ denotes the outer product of vectors and  $\mathbf{z}_k(\alpha_k, \alpha_{k+1}) \in \mathbb{R}^{n_k}$  denotes the  $(\alpha_k, \alpha_{k+1})$ th mode-2 fiber of tensor  $\mathcal{Z}_k$ . The number of parameters in TR representation is  $\mathcal{O}(dnr^2)$ , which is linear to the tensor order  $d$ .

The TR representation can also be illustrated graphically by a linear tensor network as shown in Fig. 1. A node represents a tensor (including a matrix and a vector) whose order is denoted by the number of edges. The number by an edge specifies the size of each mode (or dimension). The connection between two nodes denotes a multilinear product operator between two tensors on a specific mode. This is also called *tensor contraction*, which corresponds to the summation over the indices of that mode. It should be noted that  $\mathcal{Z}_d$  is connected to  $\mathcal{Z}_1$  by the summation over the index  $\alpha_1$ , which corresponds to the trace operation. For simplicity, we denote TR decomposition by  $\mathcal{T} = \mathfrak{R}(\mathcal{Z}_1, \mathcal{Z}_2, \dots, \mathcal{Z}_d)$ .

**Theorem 1** (Circular dimensional permutation invariance). *Let  $\mathcal{T} \in \mathbb{R}^{n_1 \times n_2 \times \dots \times n_d}$  be a  $d$ th-order tensor and its TR decomposition is given by  $\mathcal{T} = \mathfrak{R}(\mathcal{Z}_1, \mathcal{Z}_2, \dots, \mathcal{Z}_d)$ . If we define  $\overleftarrow{\mathcal{T}}^k \in \mathbb{R}^{n_{k+1} \times \dots \times n_d \times n_1 \times \dots \times n_k}$  as the circularly shifted version along the dimensions of  $\mathcal{T}$  by  $k$ , then we have  $\overleftarrow{\mathcal{T}}^k = \mathfrak{R}(\mathcal{Z}_{k+1}, \dots, \mathcal{Z}_d, \mathcal{Z}_1, \dots, \mathcal{Z}_k)$ .*

A proof of Theorem 1 is provided in Appendix A.

It should be noted that circular dimensional permutation invariance is an essential feature that distinguishes TR decomposition from TT decomposition. For TT decomposition, the product of matrices must keep a strictly sequential order, yielding that the cores for representing the same tensor with a circular dimension shifting cannot keep invariance. Hence, it is necessary to choose an optimal dimensional permutation when applying the TT decomposition.

### 3 Sequential SVDs Algorithm

We propose the first algorithm for computing the TR decomposition using  $d$  sequential SVDs. This algorithm will be called the *TR-SVD algorithm*.

**Theorem 2.** *Let us assume  $\mathcal{T}$  can be represented by a TR decomposition. If the  $k$ -unfolding matrix  $\mathbf{T}_{\langle k \rangle}$  has  $\text{Rank}(\mathbf{T}_{\langle k \rangle}) = R_{k+1}$ , then there exists a TR decomposition with TR-ranks  $\mathbf{r}$  which satisfies that  $\exists k, r_1 r_{k+1} \leq R_{k+1}$ .*

*Proof.* We can express TR decomposition in the form of  $k$ -unfolding matrix,

$$T_{\langle k \rangle}(\overline{i_1 \dots i_k}, \overline{i_{k+1} \dots i_d}) = \text{Tr} \left\{ \prod_{j=1}^k \mathbf{Z}_j(i_j) \prod_{j=k+1}^d \mathbf{Z}_j(i_j) \right\} = \left\langle \text{vec} \left( \prod_{j=1}^k \mathbf{Z}_j(i_j) \right), \text{vec} \left( \prod_{j=d}^{k+1} \mathbf{Z}_j^T(i_j) \right) \right\rangle. \quad (2)$$

It can also be rewritten as

$$T_{\langle k \rangle}(\overline{i_1 \dots i_k}, \overline{i_{k+1} \dots i_d}) = \sum_{\alpha_1 \alpha_{k+1}} Z^{\leq k}(\overline{i_1 \dots i_k}, \overline{\alpha_1 \alpha_{k+1}}) Z^{> k}(\overline{\alpha_1 \alpha_{k+1}}, \overline{i_{k+1} \dots i_d}), \quad (3)$$

where we defined the subchain by merging multiple linked cores as  $\mathbf{Z}^{\leq k}(\overline{i_1 \dots i_{k-1}}) = \prod_{j=1}^{k-1} \mathbf{Z}_j(i_j)$  and  $\mathbf{Z}^{> k}(\overline{i_{k+1} \dots i_d}) = \prod_{j=k+1}^d \mathbf{Z}_j(i_j)$ . Hence, we can obtain  $\mathbf{T}_{\langle k \rangle} = \mathbf{Z}_{(2)}^{\leq k} (\mathbf{Z}_{[2]}^{> k})^T$ , where the subchain  $\mathbf{Z}_{(2)}^{\leq k}$  is of size  $\prod_{j=1}^k n_j \times r_1 r_{k+1}$ , and  $\mathbf{Z}_{[2]}^{> k}$  is of size  $\prod_{j=k+1}^d n_j \times r_1 r_{k+1}$ . Since the rank of  $\mathbf{T}_{\langle k \rangle}$  is  $R_{k+1}$ , we can obtain  $r_1 r_{k+1} \leq R_{k+1}$ .  $\square$

According to (2) and (3), TR decomposition can be written as

$$T_{\langle 1 \rangle}(i_1, \overline{i_2 \dots i_d}) = \sum_{\alpha_1, \alpha_2} Z^{\leq 1}(i_1, \overline{\alpha_1 \alpha_2}) Z^{> 1}(\overline{\alpha_1 \alpha_2}, \overline{i_2 \dots i_d}).$$

Since the low-rank approximation of  $\mathbf{T}_{\langle 1 \rangle}$  can be obtained by the truncated SVD, which is

$$\mathbf{T}_{\langle 1 \rangle} = \mathbf{U} \Sigma \mathbf{V}^T + \mathbf{E}_1,$$

---

**Algorithm 1** TR-SVD

---

**Input:** A  $d$ th-order tensor  $\mathcal{T}$  of size  $(n_1 \times \cdots \times n_d)$  and the prescribed relative error  $\epsilon_p$ .

**Output:** Cores  $\mathcal{Z}_k, k = 1, \dots, d$  of TR decomposition and the TR-ranks  $\mathbf{r}$ .

- 1: Compute truncation threshold  $\delta_k$  for  $k = 1$  and  $k > 1$ .
  - 2: Choose one mode as the start point (e.g., the first mode) and obtain the 1-unfolding matrix  $\mathbf{T}_{(1)}$ .
  - 3: Low-rank approximation by applying  $\delta_1$ -truncated SVD:  $\mathbf{T}_{(1)} = \mathbf{U}\Sigma\mathbf{V}^T + \mathbf{E}_1$ .
  - 4: Split ranks  $r_1, r_2$  by  $\min_{r_1, r_2} \|r_1 - r_2\|$ , s. t.  $r_1 r_2 = \text{rank}_{\delta_1}(\mathbf{T}_{(1)})$ .
  - 5:  $\mathcal{Z}_1 \leftarrow \text{permute}(\text{reshape}(\mathbf{U}, [n_1, r_1, r_2]), [2, 1, 3])$ .
  - 6:  $\mathcal{Z}^{>1} \leftarrow \text{permute}(\text{reshape}(\Sigma\mathbf{V}^T, [r_1, r_2, \prod_{j=2}^d n_j]), [2, 3, 1])$ .
  - 7: **for**  $k = 2$  to  $d - 1$  **do**
  - 8:      $\mathbf{Z}^{>k-1} = \text{reshape}(\mathcal{Z}^{>k-1}, [r_k n_k, n_{k+1} \cdots n_d r_1])$ .
  - 9:     Compute  $\delta_k$ -truncated SVD:  $\mathbf{Z}^{>k-1} = \mathbf{U}\Sigma\mathbf{V}^T + \mathbf{E}_k$ .
  - 10:     $r_{k+1} \leftarrow \text{rank}_{\delta_k}(\mathbf{Z}^{>k-1})$ .
  - 11:     $\mathcal{Z}_k \leftarrow \text{reshape}(\mathbf{U}, [r_k, n_k, r_{k+1}])$ .
  - 12:     $\mathcal{Z}^{>k} \leftarrow \text{reshape}(\Sigma\mathbf{V}^T, [r_{k+1}, \prod_{j=k+1}^d n_j, r_1])$ .
  - 13: **end for**
- 

the first core  $\mathcal{Z}_1$  (i.e.,  $\mathcal{Z}^{\leq 1}$ ) of size  $r_1 \times n_1 \times r_2$  can be obtained by the proper reshaping and permutation of  $\mathbf{U}$  and the subchain  $\mathcal{Z}^{>1}$  of size  $r_2 \times \prod_{j=2}^d n_j \times r_1$  is obtained by the proper reshaping and permutation of  $\Sigma\mathbf{V}^T$ , which corresponds to the remaining  $d - 1$  dimensions of  $\mathcal{T}$ . Subsequently, we can further reshape the subchain  $\mathcal{Z}^{>1}$  as a matrix  $\mathbf{Z}^{>1} \in \mathbb{R}^{r_2 n_2 \times \prod_{j=3}^d n_j r_1}$  which thus can be written as

$$\mathbf{Z}^{>1}(\overline{\alpha_2 i_2}, \overline{i_3 \cdots i_d \alpha_1}) = \sum_{\alpha_3} Z_2(\overline{\alpha_2 i_2}, \alpha_3) \mathbf{Z}^{>2}(\alpha_3, \overline{i_3 \cdots i_d \alpha_1}).$$

By applying truncated SVD, i.e.,  $\mathbf{Z}^{>1} = \mathbf{U}\Sigma\mathbf{V}^T + \mathbf{E}_2$ , we can obtain the second core  $\mathcal{Z}_2$  of size  $(r_2 \times n_2 \times r_3)$  by appropriately reshaping  $\mathbf{U}$  and the subchain  $\mathcal{Z}^{>2}$  by proper reshaping of  $\Sigma\mathbf{V}^T$ . This procedure can be performed sequentially to obtain all  $d$  cores  $\mathcal{Z}_k, k = 1, \dots, d$ .

As proved in [14], the approximation error by using such sequential SVDs is given by

$$\|\mathcal{T} - \mathfrak{R}(\mathcal{Z}_1, \mathcal{Z}_2, \dots, \mathcal{Z}_d)\|_F \leq \sqrt{\sum_{k=1}^{d-1} \|\mathbf{E}_k\|_F^2}.$$

Hence, given a prescribed relative error  $\epsilon_p$ , the truncation threshold  $\delta$  can be set to  $\frac{\epsilon_p}{\sqrt{d-1}} \|\mathcal{T}\|_F$ . However, considering that  $\|\mathbf{E}_1\|_F$  corresponds to two ranks including both  $r_1$  and  $r_2$ , while  $\|\mathbf{E}_k\|_F, \forall k > 1$  correspond to only one rank  $r_{k+1}$ . Therefore, we modify the truncation threshold as

$$\delta_k = \begin{cases} \sqrt{2}\epsilon_p \|\mathcal{T}\|_F / \sqrt{d} & k = 1, \\ \epsilon_p \|\mathcal{T}\|_F / \sqrt{d} & k > 1. \end{cases} \quad (4)$$

A pseudocode of the TR-SVD algorithm is summarized in Alg. 1.

The cores obtained by the TR-SVD algorithm are left-orthogonal, which is  $\mathbf{Z}_{k(2)}^T \mathbf{Z}_{k(2)} = \mathbf{I}$  for  $k = 2, \dots, d - 1$ . It should be noted that TR-SVD is a non-recursive algorithm that does not need iterations for convergence. However, it might obtain different representations by choosing a different mode as the start point. This indicates that TR-ranks  $\mathbf{r}$  is not necessary to be the global optimum in TR-SVD.

## 4 Block-Wise Alternating Least-Squares (ALS) Algorithm

The ALS algorithm has been widely applied to various tensor decomposition models such as CP and Tucker decompositions [19, 20]. The main concept of ALS is optimizing one core while the other cores are fixed, and this procedure will be repeated until some convergence criterion is satisfied. Given a  $d$ th-order tensor  $\mathcal{T}$ , our goal is optimize the error function as

$$\min_{\mathcal{Z}_1, \dots, \mathcal{Z}_d} \|\mathcal{T} - \mathfrak{R}(\mathcal{Z}_1, \dots, \mathcal{Z}_d)\|_F. \quad (5)$$

According to the TR definition in (1), we have

$$\begin{aligned} T(i_1, i_2, \dots, i_d) &= \sum_{\alpha_1, \dots, \alpha_d} Z_1(\alpha_1, i_1, \alpha_2) Z_2(\alpha_2, i_2, \alpha_3) \cdots Z_d(\alpha_d, i_d, \alpha_1) \\ &= \sum_{\alpha_k, \alpha_{k+1}} \left\{ Z_k(\alpha_k, i_k, \alpha_{k+1}) Z^{\neq k}(\alpha_{k+1}, \overline{i_{k+1} \cdots i_d i_1 \cdots i_{k-1}}, \alpha_k) \right\}, \end{aligned}$$

where  $\mathbf{Z}^{\neq k}(\overline{i_{k+1} \cdots i_d i_1 \cdots i_{k-1}}) = \prod_{j=k+1}^d \mathbf{Z}_j(i_j) \prod_{j=1}^{k-1} \mathbf{Z}_j(i_j)$  denotes a slice matrix of subchain tensor by merging all cores except  $k$ th core  $\mathbf{Z}_k$ . Hence, the mode- $k$  unfolding matrix of  $\mathcal{T}$  can be expressed by

$$\mathbf{T}_{[k]}(i_k, \overline{i_{k+1} \cdots i_d i_1 \cdots i_{k-1}}) = \sum_{\alpha_k, \alpha_{k+1}} \left\{ Z_k(i_k, \overline{\alpha_k \alpha_{k+1}}) Z^{\neq k}(\overline{\alpha_k \alpha_{k+1}}, \overline{i_{k+1} \cdots i_d i_1 \cdots i_{k-1}}) \right\}.$$

By applying different mode- $k$  unfolding operations, we can obtain that  $\mathbf{T}_{[k]} = \mathbf{Z}_{k(2)} \left( \mathbf{Z}_{[2]}^{\neq k} \right)^T$ , where  $\mathbf{Z}^{\neq k}$  is a subchain obtained by merging  $d-1$  cores.

The objective function in (5) can be optimized by solving  $d$  subproblems alternatively. More specifically, having fixed all but one core, the problem reduces to a linear least squares problem, which is

$$\min_{\mathbf{Z}_{k(2)}} \left\| \mathbf{T}_{[k]} - \mathbf{Z}_{k(2)} \left( \mathbf{Z}_{[2]}^{\neq k} \right)^T \right\|_F, \quad k = 1, \dots, d.$$

Here, we propose a computationally efficient block-wise ALS (BALS) algorithm by utilizing truncated SVD, which facilitates the self-adaptation of ranks. The main idea is to perform the blockwise optimization followed by the separation of a block into individual cores. To achieve this, we consider merging two linked cores, e.g.,  $\mathbf{Z}_k, \mathbf{Z}_{k+1}$ , into a block (or subchain)  $\mathbf{Z}^{(k, k+1)} \in \mathbb{R}^{r_k \times n_k n_{k+1} \times r_{k+2}}$ . Thus, the subchain  $\mathbf{Z}^{(k, k+1)}$  can be optimized while leaving all cores except  $\mathbf{Z}_k, \mathbf{Z}_{k+1}$  fixed. Subsequently, the subchain  $\mathbf{Z}^{(k, k+1)}$  can be reshaped into  $\tilde{\mathbf{Z}}^{(k, k+1)} \in \mathbb{R}^{r_k n_k \times n_{k+1} r_{k+2}}$  and separated into a left-orthonormal core  $\mathbf{Z}_k$  and  $\mathbf{Z}_{k+1}$  by a truncated SVD:

$$\tilde{\mathbf{Z}}^{(k, k+1)} = \mathbf{U} \mathbf{\Sigma} \mathbf{V}^T = \mathbf{Z}_{k(2)} \mathbf{Z}_{k+1(1)}, \quad (6)$$

where  $\mathbf{Z}_{k(2)} \in \mathbb{R}^{r_k n_k \times r_{k+1}}$  is the 2-unfolding matrix of core  $\mathbf{Z}_k$ , which can be set to  $\mathbf{U}$ , while  $\mathbf{Z}_{k+1(1)} \in \mathbb{R}^{r_{k+1} \times n_{k+1} r_{k+2}}$  is the 1-unfolding matrix of core  $\mathbf{Z}_{k+1}$ , which can be set to  $\mathbf{\Sigma} \mathbf{V}^T$ . This procedure thus moves on to optimize the next block cores  $\mathbf{Z}^{(k+1, k+2)}, \dots, \mathbf{Z}^{(d-1, d)}, \mathbf{Z}^{(d, 1)}$  successively in the similar way. Note that since the TR model is circular, the  $d$ th core can also be merged with the first core yielding the block core  $\mathbf{Z}^{(d, 1)}$ .

The key advantage of our BALS algorithm is the rank adaptation ability which can be achieved simply by separating the block core into two cores via truncated SVD, as shown in (6). The truncated rank  $r_{k+1}$  can be chosen such that the approximation error is below a certain threshold. One possible choice is to use the same threshold as in the TR-SVD algorithm, i.e.,  $\delta_k$  described in (4). However, the empirical experience shows that this threshold often leads to overfitting and the truncated rank is higher than the optimal rank. This is because the updated block  $\mathbf{Z}^{(k, k+1)}$  during ALS iterations is not a closed form solution and many iterations are necessary for convergence. To relieve this problem, we choose the truncation threshold based on both the current and the desired approximation errors, which is

$$\delta = \max \left\{ \epsilon \|\mathcal{T}\|_F / \sqrt{d}, \epsilon_p \|\mathcal{T}\|_F / \sqrt{d} \right\}.$$

A pseudo code of the BALS algorithm is described in Alg. 2.

## 5 Properties of TR Representation

By assuming that tensor data have been already represented as TR decompositions, i.e., a sequence of third-order cores, we justify and demonstrate that the basic operations on tensors, such as the *addition*, *multilinear product*, *Hadamard product*, *inner product* and *Frobenius norm*, can be performed efficiently by the appropriate operations on each individual cores. We have the following theorems:

---

**Algorithm 2** TR-BALS
 

---

**Input:** A  $d$ -dimensional tensor  $\mathcal{T}$  of size  $(n_1 \times \dots \times n_d)$  and the prescribed relative error  $\epsilon_p$ .

**Output:** Cores  $\mathcal{Z}_k$  and TR-ranks  $r_k$ ,  $k = 1, \dots, d$ .

- 1: Initialize  $r_k = 1$  for  $k = 1, \dots, d$ .
- 2: Initialize  $\mathcal{Z}_k \in \mathbb{R}^{r_k \times n_k \times r_{k+1}}$  for  $k = 1, \dots, d$ .
- 3: **repeat**  $k \in \text{circular}\{1, 2, \dots, d\}$ ;
- 4:   Compute the subchain  $\mathcal{Z}^{\neq(k, k+1)}$ .
- 5:   Obtain the mode-2 unfolding matrix  $\mathbf{Z}_{[2]}^{\neq(k, k+1)}$  of size  $\prod_{j=1}^d n_j / (n_k n_{k+1}) \times r_k r_{k+2}$ .
- 6:    $\mathbf{Z}_{(2)}^{(k, k+1)} \leftarrow \arg \min \left\| \mathbf{T}_{[k]} - \mathbf{Z}_{(2)}^{(k, k+1)} \left( \mathbf{Z}_{[2]}^{\neq(k, k+1)} \right)^T \right\|_F$ .
- 7:   Tensorization of mode-2 unfolding matrix

$$\mathcal{Z}^{(k, k+1)} \leftarrow \text{folding}(\mathbf{Z}_{(2)}^{(k, k+1)}).$$

- 8:   Reshape the block core by

$$\tilde{\mathcal{Z}}^{(k, k+1)} \leftarrow \text{reshape}(\mathcal{Z}^{(k, k+1)}, [r_k n_k \times n_{k+1} r_{k+2}]).$$

- 9:   Low-rank approximation by  $\delta$ -truncated SVD  $\tilde{\mathcal{Z}}^{(k, k+1)} = \mathbf{U} \Sigma \mathbf{V}^T$ .
  - 10:    $\mathcal{Z}_k \leftarrow \text{reshape}(\mathbf{U}, [r_k, n_k, r_{k+1}])$ .
  - 11:    $\mathcal{Z}_{k+1} \leftarrow \text{reshape}(\Sigma \mathbf{V}^T, [r_{k+1}, n_{k+1}, r_{k+2}])$ .
  - 12:    $r_{k+1} \leftarrow \text{rank}_\delta(\tilde{\mathcal{Z}}^{(k, k+1)})$ .
  - 13:    $k \leftarrow k + 1$ .
  - 14: **until** The desired approximation accuracy is achieved, i.e.,  $\epsilon \leq \epsilon_p$ .
- 

**Theorem 3.** Let  $\mathcal{T}_1$  and  $\mathcal{T}_2$  be  $d$ th-order tensors of size  $n_1 \times \dots \times n_d$ . If TR decompositions of these two tensors are  $\mathcal{T}_1 = \mathfrak{R}(\mathcal{Z}_1, \dots, \mathcal{Z}_d)$  where  $\mathcal{Z}_k \in \mathbb{R}^{r_k \times n_k \times r_{k+1}}$  and  $\mathcal{T}_2 = \mathfrak{R}(\mathcal{Y}_1, \dots, \mathcal{Y}_d)$  where  $\mathcal{Y}_k \in \mathbb{R}^{s_k \times n_k \times s_{k+1}}$ , then the addition of these two tensors,  $\mathcal{T}_3 = \mathcal{T}_1 + \mathcal{T}_2$ , can also be represented in the TR format given by  $\mathcal{T}_3 = \mathfrak{R}(\mathcal{X}_1, \dots, \mathcal{X}_d)$ , where  $\mathcal{X}_k \in \mathbb{R}^{q_k \times n_k \times q_{k+1}}$  and  $q_k = r_k + s_k$ . Each core  $\mathcal{X}_k$  can be computed by

$$\mathbf{X}_k(i_k) = \begin{pmatrix} \mathbf{Z}_k(i_k) & 0 \\ 0 & \mathbf{Y}_k(i_k) \end{pmatrix}, \quad i_k = 1, \dots, n_k, \quad k = 1, \dots, d. \quad (7)$$

A proof of Theorem 3 is provided in Appendix B. Note that the sizes of new cores are increased and not optimal in general. This problem can be solved by the rounding procedure [14].

**Theorem 4.** Let  $\mathcal{T} \in \mathbb{R}^{n_1 \times \dots \times n_d}$  be a  $d$ th-order tensor whose TR representation is  $\mathcal{T} = \mathfrak{R}(\mathcal{Z}_1, \dots, \mathcal{Z}_d)$  and  $\mathbf{u}_k \in \mathbb{R}^{n_k}$ ,  $k = 1, \dots, d$  be a set of vectors, then the multilinear products, denoted by  $c = \mathcal{T} \times_1 \mathbf{u}_1^T \times_2 \dots \times_d \mathbf{u}_d^T$ , can be computed by the multilinear product on each cores, which is

$$c = \mathfrak{R}(\mathbf{X}_1, \dots, \mathbf{X}_d) \text{ where } \mathbf{X}_k = \sum_{i_k=1}^{n_k} \mathbf{Z}_k(i_k) u_k(i_k). \quad (8)$$

A proof of Theorem 4 is provided in Appendix C. It should be noted that the computational complexity in the original tensor form is  $\mathcal{O}(dn^d)$ , while it reduces to  $\mathcal{O}(dnr^2 + dr^3)$  that is linear to tensor order  $d$  by using TR representation.

**Theorem 5.** Let  $\mathcal{T}_1$  and  $\mathcal{T}_2$  be  $d$ th-order tensors of size  $n_1 \times \dots \times n_d$ . If the TR decompositions of these two tensors are  $\mathcal{T}_1 = \mathfrak{R}(\mathcal{Z}_1, \dots, \mathcal{Z}_d)$  where  $\mathcal{Z}_k \in \mathbb{R}^{r_k \times n_k \times r_{k+1}}$  and  $\mathcal{T}_2 = \mathfrak{R}(\mathcal{Y}_1, \dots, \mathcal{Y}_d)$  where  $\mathcal{Y}_k \in \mathbb{R}^{s_k \times n_k \times s_{k+1}}$ , then the Hadamard product of these two tensors,  $\mathcal{T}_3 = \mathcal{T}_1 \otimes \mathcal{T}_2$ , can also be represented in the TR format given by  $\mathcal{T}_3 = \mathfrak{R}(\mathcal{X}_1, \dots, \mathcal{X}_d)$ , where  $\mathcal{X}_k \in \mathbb{R}^{q_k \times n_k \times q_{k+1}}$  and  $q_k = r_k s_k$ . Each core  $\mathcal{X}_k$  can be computed by

$$\mathbf{X}_k(i_k) = \mathbf{Z}_k(i_k) \otimes \mathbf{Y}_k(i_k), \quad k = 1, \dots, d. \quad (9)$$

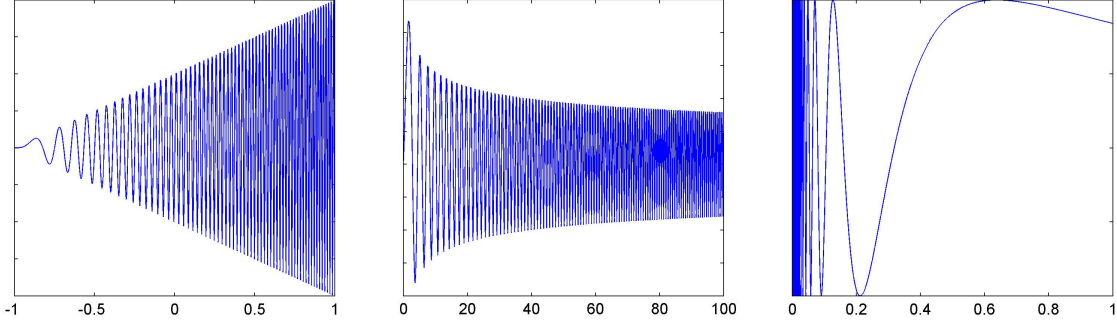


Figure 2: Highly oscillated functions. The left panel is  $f_1(x) = (x + 1) \sin(100(x + 1)^2)$ . The middle panel is Airy function:  $f_2(x) = x^{-\frac{1}{4}} \sin(\frac{2}{3}x^{\frac{3}{2}})$ . The right panel is Chirp function  $f_3(x) = \sin \frac{x}{4} \cos(x^2)$ .

Table 1: The functional data  $f_1(x), f_2(x), f_3(x)$  is tensorized to 10th-order tensor ( $4 \times 4 \times \dots \times 4$ ). In the table,  $\epsilon, \bar{r}, N_p$  denote relative error, average rank, and the total number of parameters, respectively.

	$f_1(x)$				$f_2(x)$			
	$\epsilon$	$\bar{r}$	$N_p$	Time (s)	$\epsilon$	$\bar{r}$	$N_p$	Time (s)
TT-SVD	3e-4	4.4	1032	0.17	3e-4	5	1360	0.16
TR-SVD	3e-4	4.4	1032	0.17	3e-4	5	1360	0.28
TR-BALS	9e-4	4.3	1052	4.6	8e-4	4.9	1324	5.7
	$f_3(x)$				$f_1(x) + \mathcal{N}(0, \sigma), SNR = 60dB$			
	$\epsilon$	$\bar{r}$	$N_p$	Time (s)	$\epsilon$	$\bar{r}$	$N_p$	Time (s)
TT-SVD	3e-4	3.7	680	0.16	1e-3	16.6	13064	0.5
TR-SVD	5e-4	3.6	668	0.15	1e-3	9.7	4644	0.4
TR-BALS	5e-4	3.7	728	3.4	1e-3	4.2	1000	6.1

A proof of Theorem 5 is provided in Appendix D. Furthermore, one can compute the *inner product* of two tensors in TR representations. For two tensors  $\mathcal{T}_1$  and  $\mathcal{T}_2$ , it is defined as  $\langle \mathcal{T}_1, \mathcal{T}_2 \rangle = \sum_{i_1, \dots, i_d} T_3(i_1, \dots, i_d)$ , where  $\mathcal{T}_3 = \mathcal{T}_1 \otimes \mathcal{T}_2$ . Thus, the inner product can be computed by applying the Hadamard product and then computing the multilinear product between  $\mathcal{T}_3$  and vectors of all ones, i.e.,  $\mathbf{u}_k = \mathbf{1}, k = 1, \dots, d$ . In contrast to  $\mathcal{O}(n^d)$  in the original tensor form, the computational complexity is equal to  $\mathcal{O}(dnq^2 + dq^3)$  that is linear to  $d$  by using TR representation. Similarly, we can also compute the *Frobenius norm*  $\|\mathcal{T}\|_F = \sqrt{\langle \mathcal{T}, \mathcal{T} \rangle}$  in the TR representation.

## 6 Experimental Results

In this section, we experimentally demonstrate the usefulness of the proposed approach.

### 6.1 Numerical Illustration

We consider highly oscillating functions that can be approximated well by a low-rank TT format [21], as shown in Fig. 2. We firstly tensorize the functional vector resulting in a  $d$ th-order tensor of size  $n_1 \times n_2 \times \dots \times n_d$ , where isometric size is usually preferred, i.e.,  $n_1 = n_2 = \dots = n_d = n$ , with the total number of elements denoted by  $N = n^d$ . The error bound (tolerance), denoted by  $\epsilon_p = 10^{-3}$ , is given as the stopping criterion for all compared algorithms. As shown in Table 1, TR-SVD and TR-BALS can obtain comparable results with TT-SVD while outperform TT-SVD when noise is involved. These results indicate that TR representation is more robust to noise than TT representation.

It should be noted that TT representation has the property that  $r_1 = r_{d+1} = 1$  and  $r_k, k = 2, \dots, d-1$  are bounded by the rank of  $k$ -unfolding matrix of  $\mathbf{T}_{(k)}$ , which limits its generalization ability and consistency when the tensor modes have been shifted or permuted. To demonstrate this, we consider shifting the dimensions

Table 2: The results under different shifts of dimensions on functional data  $f_2(x)$  with error bound set at  $10^{-3}$ . For the 10th-order tensor, all 9 dimension shifts were considered to compare the average rank  $\bar{r}$ .

	$\bar{r}$								
	1	2	3	4	5	6	7	8	9
TT-SVD	5.2	5.8	6	6.2	7	7	8.5	14.6	8.4
TR-SVD	5.2	5.8	5.9	6.2	9.6	10	14	12.7	6.5
TR-BALS	5	4.9	5	4.9	4.9	5	5	4.8	4.9

Table 3: The comparisons of different algorithms on Coil-100 dataset.  $\epsilon$ ,  $r_{max}$ ,  $\bar{r}$  denote relative error, the maximum rank and the average rank, respectively.

	$\epsilon$	$r_{max}$	$\bar{r}$	Acc. (%)	Acc. (%)
				( $\rho = 50\%$ )	( $\rho = 10\%$ )
TT-SVD	0.19	67	47.3	99.05	89.11
	0.28	23	16.3	98.99	88.45
	0.37	8	6.3	96.29	86.02
	0.46	3	2.7	47.78	44.00
TR-SVD	0.19	23	12.0	99.14	89.29
	0.28	10	6.0	99.19	89.89
	0.36	5	3.5	98.51	88.10
	0.43	3	2.3	83.43	73.20

of  $\mathcal{T}$  of size  $n_1 \times \dots \times n_d$  by  $k$  times leading to  $\overleftarrow{\mathcal{T}}^k$  of size  $n_{k+1} \times \dots \times n_d \times n_1 \times \dots \times n_k$ . As shown in Table 2, the average TT-ranks are varied dramatically along with the different shifts. In particular, when  $k = 8$ ,  $\bar{r}_{tt}$  becomes 14.6, resulting in a large number of parameters  $N_p = 10376$ . In contrast to TT, TR-BALS can obtain consistent and compact representation.

## 6.2 COIL-100 dataset

The Columbia Object Image Libraries (COIL)-100 dataset [22] contains 7200 color images of 100 objects (72 images per object) with different reflectance and complex geometric characteristics. Each image can be represented by a 3rd-order tensor of size  $128 \times 128 \times 3$  and then is downsampled to  $32 \times 32 \times 3$ . Hence, the dataset can be finally organized as a 4th-order tensor of size  $32 \times 32 \times 3 \times 7200$ . The number of features is determined by  $r_4 \times r_1$ , while the flexibility of subspace bases is determined by  $r_2, r_3$ . Subsequently, we apply the K-nearest neighbor (KNN) classifier with  $K=1$  for classification. For detailed comparisons, we randomly select a certain ratio  $\rho = 50\%$  or  $\rho = 10\%$  samples as the training set and the rest as the test set. The classification performance is averaged over 10 times of random splitting. In Table 3,  $r_{max}$  of TR decompositions is much smaller than that of TT-SVD. It should be noted that TR representation, as compared to TT, can obtain more compact and discriminant representations.

We have conducted an additional experiment on video classifications (see detailed results in the Appendix).

## 7 Conclusion

We have proposed a novel tensor decomposition model, which provides an efficient representation for a very high-order tensor by a sequence of low-dimensional cores. The number of parameters in our model scales only linearly to the tensor order. To optimize the latent cores, we have presented two different algorithms: TR-SVD is a non-recursive algorithm that is stable and efficient, while TR-BALS can learn a more compact representation with adaptive TR-ranks. Furthermore, we have investigated the properties on how the basic multilinear algebra can be performed efficiently by operations over TR representations (i.e., cores), which provides a powerful framework for processing large-scale data. The experimental results verified the effectiveness of our proposed algorithms.



## References

- [1] A. Anandkumar, R. Ge, D. J. Hsu, S. M. Kakade, and M. Telgarsky, “Tensor decompositions for learning latent variable models.” *Journal of Machine Learning Research*, vol. 15, no. 1, pp. 2773–2832, 2014.
- [2] B. Romera-Paredes, H. Aung, N. Bianchi-Berthouze, and M. Pontil, “Multilinear multitask learning,” in *International Conference on Machine Learning*, 2013, pp. 1444–1452.
- [3] H. Kanagawa, T. Suzuki, H. Kobayashi, N. Shimizu, and Y. Tagami, “Gaussian process nonparametric tensor estimator and its minimax optimality,” in *International Conference on Machine Learning (ICML2016)*, 2016, pp. 1632–1641.
- [4] F. Cong, Q.-H. Lin, L.-D. Kuang, X.-F. Gong, P. Astikainen, and T. Ristaniemi, “Tensor decomposition of EEG signals: a brief review,” *Journal of neuroscience methods*, vol. 248, pp. 59–69, 2015.
- [5] G. Zhou, Q. Zhao, Y. Zhang, T. Adali, S. Xie, and A. Cichocki, “Linked component analysis from matrices to high-order tensors: Applications to biomedical data,” *Proceedings of the IEEE*, vol. 104, no. 2, pp. 310–331, 2016.
- [6] R. Bro, “PARAFAC. Tutorial and applications,” *Chemometrics and intelligent laboratory systems*, vol. 38, no. 2, pp. 149–171, 1997.
- [7] J. Goulart, M. Boizard, R. Boyer, G. Favier, and P. Comon, “Tensor cp decomposition with structured factor matrices: Algorithms and performance,” *IEEE Journal of Selected Topics in Signal Processing*, 2015.
- [8] Q. Zhao, L. Zhang, and A. Cichocki, “Bayesian CP factorization of incomplete tensors with automatic rank determination,” *IEEE Transactions on Pattern Analysis and Machine Intelligence*, vol. 37, no. 9, pp. 1751–1763, 2015.
- [9] L. R. Tucker, “Some mathematical notes on three-mode factor analysis,” *Psychometrika*, vol. 31, no. 3, pp. 279–311, 1966.
- [10] L. De Lathauwer, B. De Moor, and J. Vandewalle, “On the best rank-1 and rank-(R1,R2, . . . ,RN) approximation of higher-order tensors,” *SIAM J. Matrix Anal. Appl.*, vol. 21, pp. 1324–1342, 2000.
- [11] Z. Xu, F. Yan, and A. Qi, “Infinite Tucker decomposition: Nonparametric Bayesian models for multiway data analysis,” in *Proceedings of the 29th International Conference on Machine Learning (ICML-12)*, 2012, pp. 1023–1030.
- [12] Q. Wu, L. Zhang, and A. Cichocki, “Multifactor sparse feature extraction using convolutive nonnegative tucker decomposition,” *Neurocomputing*, vol. 129, pp. 17–24, 2014.
- [13] A. Cichocki, N. Lee, I. Oseledets, A.-H. Phan, Q. Zhao, D. P. Mandic *et al.*, “Tensor networks for dimensionality reduction and large-scale optimization: Part 1 low-rank tensor decompositions,” *Foundations and Trends® in Machine Learning*, vol. 9, no. 4-5, pp. 249–429, 2016.
- [14] I. V. Oseledets, “Tensor-train decomposition,” *SIAM Journal on Scientific Computing*, vol. 33, no. 5, pp. 2295–2317, 2011.
- [15] A. Novikov, D. Podoprikin, A. Osokin, and D. P. Vetrov, “Tensorizing neural networks,” in *Advances in Neural Information Processing Systems*, 2015, pp. 442–450.
- [16] E. Stoudenmire and D. J. Schwab, “Supervised learning with tensor networks,” in *Advances in Neural Information Processing Systems 29*, D. D. Lee, M. Sugiyama, U. V. Luxburg, I. Guyon, and R. Garnett, Eds. Curran Associates, Inc., 2016, pp. 4799–4807. [Online]. Available: <http://papers.nips.cc/paper/6211-supervised-learning-with-tensor-networks.pdf>
- [17] J. A. Bengua, H. N. Phien, and H. D. Tuan, “Optimal feature extraction and classification of tensors via matrix product state decomposition,” in *2015 IEEE International Congress on Big Data*, June 2015, pp. 669–672.

- [18] I. Oseledets and E. Tyrtyshnikov, "TT-cross approximation for multidimensional arrays," *Linear Algebra and its Applications*, vol. 432, no. 1, pp. 70–88, 2010.
- [19] T. Kolda and B. Bader, "Tensor decompositions and applications," *SIAM Review*, vol. 51, no. 3, pp. 455–500, 2009.
- [20] S. Holtz, T. Rohwedder, and R. Schneider, "The alternating linear scheme for tensor optimization in the tensor train format," *SIAM J. Scientific Computing*, vol. 34, no. 2, 2012.
- [21] B. N. Khoromskij, "Tensor numerical methods for multidimensional PDEs: theoretical analysis and initial applications," *ESAIM: Proceedings and Surveys*, vol. 48, pp. 1–28, 2015.
- [22] S. Nayar, S. Nene, and H. Murase, "Columbia object image library (coil 100)," *Department of Comp. Science, Columbia University, Tech. Rep. CUCS-006-96*, 1996.
- [23] I. Laptev and T. Lindeberg, "Local descriptors for spatio-temporal recognition," in *Spatial Coherence for Visual Motion Analysis*. Springer, 2006, pp. 91–103.

## A Proof of Theorem 1

*Proof.* It is obvious that (1) can be rewritten as

$$\begin{aligned} T(i_1, i_2, \dots, i_d) &= \text{Tr}(\mathbf{Z}_2(i_2), \mathbf{Z}_3(i_3), \dots, \mathbf{Z}_d(i_d), \mathbf{Z}_1(i_1)) \\ &= \dots = \text{Tr}(\mathbf{Z}_d(i_d), \mathbf{Z}_1(i_1), \dots, \mathbf{Z}_{d-1}(i_{d-1})). \end{aligned}$$

Therefore, we have  $\overleftarrow{\mathcal{T}}^k = \Re(\mathcal{Z}_{k+1}, \dots, \mathcal{Z}_d, \mathcal{Z}_1, \dots, \mathcal{Z}_k)$ .  $\square$

## B Proof of Theorem 3

*Proof.* According to the definition of TR decomposition, and the cores shown in (7), the  $(i_1, \dots, i_d)$ th element of tensor  $\mathcal{T}_3$  can be written as

$$T_3(i_1, \dots, i_d) = \text{Tr} \begin{pmatrix} \prod_{k=1}^d \mathbf{Z}_k(i_k) & 0 \\ 0 & \prod_{k=1}^d \mathbf{Y}_k(i_k) \end{pmatrix} = \text{Tr} \left( \prod_{k=1}^d \mathbf{Z}_k(i_k) \right) + \text{Tr} \left( \prod_{k=1}^d \mathbf{Y}_k(i_k) \right).$$

Hence, the *addition* of tensors in the TR format can be performed by merging of their cores.  $\square$

## C Proof of Theorem 4

*Proof.* The *multilinear product* between a tensor and vectors can be expressed by

$$\begin{aligned} c &= \sum_{i_1, \dots, i_d} T(i_1, \dots, i_d) u_1(i_1) \cdots u_d(i_d) = \sum_{i_1, \dots, i_d} \text{Tr} \left( \prod_{k=1}^d \mathbf{Z}_k(i_k) \right) u_1(i_1) \cdots u_d(i_d) \\ &= \text{Tr} \left( \prod_{k=1}^d \left( \sum_{i_k=1}^{n_k} \mathbf{Z}_k(i_k) u_k(i_k) \right) \right). \end{aligned}$$

Thus, it can be written as a TR decomposition shown in (8) where each core  $\mathbf{X}_k \in \mathbb{R}^{r_k \times r_{k+1}}$  becomes a matrix. The computational complexity is equal to  $\mathcal{O}(dnr^2)$ .  $\square$

## D Proof of Theorem 5

*Proof.* Each element in tensor  $\mathcal{T}_3$  can be written as

$$\begin{aligned} T_3(i_1, \dots, i_d) &= \text{Tr} \left( \prod_{k=1}^d \mathbf{Z}_k(i_k) \right) \text{Tr} \left( \prod_{k=1}^d \mathbf{Y}_k(i_k) \right) = \text{Tr} \left\{ \left( \prod_{k=1}^d \mathbf{Z}_k(i_k) \right) \otimes \left( \prod_{k=1}^d \mathbf{Y}_k(i_k) \right) \right\} \\ &= \text{Tr} \left\{ \prod_{k=1}^d \left( \mathbf{Z}_k(i_k) \otimes \mathbf{Y}_k(i_k) \right) \right\}. \end{aligned}$$

Hence,  $\mathcal{T}_3$  can be also represented as TR format with its cores computed by (9), which costs  $\mathcal{O}(dnq^2)$ .  $\square$

## E KTH video dataset

We test the TR representation for KTH video database [23] containing six types of human actions (walking, jogging, running, boxing, hand waving and hand clapping) performed several times by 25 subjects in four different scenarios: outdoors, outdoors with scale variation, outdoors with different clothes and indoors as illustrated in Fig. 3. There are 600 video sequences for each combination of 25 subjects, 6 actions and 4 scenarios. Each video sequence was downsampled to  $20 \times 20 \times 32$ . Finally, we can organize the dataset as a



Figure 3: Video dataset consists of six types of human actions performed by 25 subjects in four different scenarios. From the top to bottom, six video examples corresponding to each type of actions are shown.

Table 4: The comparisons of different algorithms on KTH dataset.  $\epsilon$  denotes the obtained relative error;  $r_{max}$  denotes maximum rank;  $\bar{r}$  denotes the average rank; and Acc. is the classification accuracy.

	$\epsilon$	$r_{max}$	$\bar{r}$	Acc. ( $5 \times 5$ -fold)
CP-ALS	0.20	300	300	80.8 %
	0.30	40	40	79.3 %
	0.40	10	10	66.8 %
TT-SVD	0.20	139	78.0	84.8 %
	0.29	38	27.3	83.5 %
	0.38	14	9.3	67.8 %
TR-SVD	0.20	99	34.2	78.8 %
	0.29	27	12.0	87.7 %
	0.37	10	5.8	72.4 %

tensor of size  $20 \times 20 \times 32 \times 600$ . For extensive comparisons, we choose different error bound  $\epsilon_p \in \{0.2, 0.3, 0.4\}$ . In Table 4, we can see that TR representations achieve better compression ratio reflected by smaller  $r_{max}, \bar{r}$  than that of TT-SVD, while TT-SVD achieves better compression ratio than CP-ALS. For instance, when  $\epsilon \approx 0.2$ , CP-ALS requires  $r_{max} = 300, \bar{r} = 300$ ; TT-SVD requires  $r_{max} = 139, \bar{r} = 78$ , while TR-SVD only requires  $r_{max} = 99, \bar{r} = 34.2$ . For classification performance, we observe that the best accuracy ( $5 \times 5$ -fold cross validation) achieved by CP-ALS, TT-SVD, TR-SVD are 80.8%, 84.8%, 87.7%, respectively. Note that these classification performances might not be the state-of-the-art on this dataset, we mainly focus on the comparisons of representation ability among CP, TT, and TR decomposition frameworks. To obtain the best performance, we may apply the powerful feature extraction methods to TT or TR representations of dataset. It should be noted that TR decompositions achieve the best classification accuracy when  $\epsilon = 0.29$ , while TT-SVD and CP-ALS achieve their best classification accuracy when  $\epsilon = 0.2$ . This indicates that TR decomposition can preserve more discriminant information even when the approximation error is relatively high. This experiment demonstrates that TR decompositions are effective for unsupervised feature representation due to their flexibility of TR-ranks and high compression ability.